Research Article

Journal of PeptideScience

Received: 5 January 2009 Revised: 27 May 2009 Accepted: 28 May 2009 Published online in Wiley Interscience: 29 July 2009

(www.interscience.com) DOI 10.1002/psc.1155

Effect of Leucine and Lysine substitution on the antimicrobial activity and evaluation of the mechanism of the HPA3NT3 analog peptide‡

Ramamourthy Gopal,[a] Seong-Cheol Park,[a] Kyeoung-Ju Ha,[b] Seung Joo Cho,[c] Si Wouk Kim,[d] Peter I. Song,[e] Jae-Woon Nah,[f] Yoonkyung Park[a,g]* and Kyung-Soo Hahm[a,c]*

In this study, a HPA3NT3-analog (FKKLKKLFKKILKLK-NH_2) peptide was designed. In this analog, two Trp residues (positions 12, 14) were replaced with Leu, and Arg and Asn (positions 3, 13) were replaced with Lys to investigate the role of amino acid substitution and increased cationicity on antimicrobial and hemolytic activities. In fungal and Gram-negative bacterial cells, HPA3NT3-analog activity was unchanged or slightly enhanced when compared to the HPA3NT3 peptide. In addition, a twofold decrease in activity against Gram-positive bacteria was observed. The HPA3NT3-analog also induced less hemolysis (4.2%) than the HPA3NT3 peptide (71%) at 200 μM. Circular dichroism (CD) spectra revealed that the HPA3NT3-analog peptide had an unordered structure in buffer and egg yolk L-2-phosphatidyl choline (EYPC), but adapted an α-helical conformation in 50% 2,2,2-trifluoroethanol (TFE) and negatively charged egg yolk L-2-phosphatidyl glycerol (EYPG), while the parent peptide showed an ordered structure in the EYPC. Additionally, the HPA3NT3-analog peptide induced the leakage of calcein from egg yolk L-2-phosphatidyl ethanolamine (EYPE)/EYPG (7 : 3 w/w) large unilamellar vesicles (LUVs); however, the activity was slightly weaker than that of the HPA3NT3 peptide. The molecular dynamics (MD) structures revealed that the amino acid substitutions induced a significant variation in peptide structure. These results suggest that the substitutions of Arg and Asn with Lys and two Trp with Leu resulted in small changes in HPA3NT3-analog activity and significant decreases in hemolytic activity.

Keywords: antimicrobial activity; hemolysis; HPA3NT3-analog peptide; leakage of calcein; molecular dynamics

Introduction

Cationic AMPs are produced by a wide variety of living organisms. AMPs are considered to be a new class of clinical antibiotics because of their broad spectrum activity against a range of microorganisms, including antibiotic resistant strains. In addition, AMPs are recognized as a component of innate immunity [1]. Most cationic AMPs are generally 13–50 amino acids in length, contain 2–9 basic residues (Arg or Lys) and approximately 50% hydrophobic amino acids [2]. These peptides adopt a well defined amphipathic structure in lipid membrane environments such as α-helices, β-sheets, extended peptides or looped peptides [3]. Their cationic and hydrophobic side chains were located on opposite faces of the amphipathic structure. It has also been proposed that they can form electrostatic and hydrophobic interactions with negatively charged anionic lipid headgroups [1].

However, it has been shown that the side chains of Arg and Trp residues of several cationic AMPs are not selective for bacterial membranes [4–6]. For example, the guanidinium group of Arg and a bulky indole side chain of Trp interact strongly with zwitterionic phospholipids membranes, thereby promoting eukaryotic cell toxicity [5,6]. As a result, synthetic cationic peptides could be selectively designed for bacterial cells based on their amino acid combination, charge, hydrophobicity/hydrophilicity, and helicity [7,8]. Keeping these points in mind, we designed an analog peptide (HPA3NT3-analog) from a truncated peptide HPA3NT3 (parent). This parent peptide is an analog of HP (2–20), which was derived

* *Correspondence to: Yoonkyung Park and Kyung-Soo Hahm, Research Center for Proteineous Materials (RCPM), Chosun University, 375 Seosuk-Dong, Dong-Ku, Gwangju 501-759, Korea.*
E-mail: y_k_park@chosun.ac.kr; kshahm@chosun.ac.kr

a *Research Center for Proteineous Materials (RCPM), Chosun University, Gwangju, Korea*

b *Faculty of Mobilecontents, Daegu Hanny University, Gyeongsan-si, Korea*

c *Department of Cellular and Molecular Medicine, School of Medicine, Chosun University, Gwangju, Korea*

d *Department of Environmental Engineering, Chosun University, Gwangju, Korea*

e *Department of Dermatology, University of Arkansas for Medical Sciences, 4301 West Markham, slot 576 Little Rock, AR 72205, USA*

f *Department of Polymer Science and Engineering, Sunchon National University, 315 Maegok, Suncheon, Korea*

g *Department of Biotechnology and BK21 Research Team for Protein Activity Control, Chosun University, Gwangju, Korea*

‡ *Special issue devoted to contributions presented at the 1st Italy-Korea Symposium on Antimicrobial Peptides, 24–25 July 2008.*

Abbreviations used: *AMPs, antimicrobial peptides; CD, circular dichroism; CH, cholesterol; EYPC, egg yolk L-α-phosphatidylcholine; EYPE, egg yolk L-α-phosphatidylethanolamine; EYPG, egg yolk L-2-phosphatidyl glycerol; Fmoc, 9-fluorenyl-methoxycarbonyl; hRBCs, human red blood cells; LUVs, large unilamellar vesicles; MD, molecular dynamics; MTT, 3-(4,5-dimethyl-2-thiazolyl)-2,5-diphenyl-2H-tetrazolium bromide; PBS, phosphate buffer saline; RMSD, root mean square deviation; TFE, 2,2,2-trifluoroethanol.*

from the *N*-terminus of the *Helicobacter pylori* ribosomal protein L1 [9–11].

Here we report that an increase of cationicity occurs in response to substitution of Arg and Asn with Lys and *C*-terminal amidation, and the nature of the hydrophobic face is altered by substitution of two Trp with Leu in the HPA3NT3-analog, and that these changes lead to a decrease in hemolysis. We examined the peptide secondary structure in the model lipids by CD spectroscopy and the mechanism of action by fluorescent dye leakage. Finally, computer modeling and MD structures of these peptides were generated to determine the influence of amino acid substitutions on the HPA3NT3-analog peptide.

Materials and Methods

Peptide Synthesis

The peptides, HPA3NT3 (FKRLKKLFKKIWNWK) and HPA3NT3-analog (FKKLKKLFKKILKLK-NH_2), were synthesized by the solid-phase method using Fmoc chemistry [12]. The crude peptides were then purified using reverse phase preparative HPLC on a Waters 15 μm deltapak C_{18} column (19 × 30 cm). Next, the purified peptides were hydrolyzed with 6 N HCl at 110 °C for 22 h, after which they were dried in a vacuum. The amino acid residues were then dissolved in 0.02 N HCl and evaluated using an amino acid analyzer (Hitachi model, 8500 A, Hitachi, Tokyo, Japan). Finally, the peptide concentration was determined by amino acid analysis.

Antibacterial Activity

The antibacterial activities of the peptides against Gram-negative bacteria (*Escherichia coli*, Korean collection for type culture (KCTC) 1682; *Salmonella typhimurium*, KCTC 1926; and *Pseudomonas aeruginosa*, KCTC 1637) and Gram-positive bacteria (*Staphylococcus aureus*, KCTC 1621; *Bacillus subtilis,* KCTC 1918 and *Listeria monocytogenes,* KCTC 3710) were examined using the microbroth dilution method [13] or sterile 96-well plates. Aliquots of bacterial suspensions (50 μl) in mid-log phase at a concentration of 2×10^6 colony forming units (CFU)/ml in culture medium (1% peptone) were added to each well containing 50 μl of peptide solution that had been twofold serially diluted in buffer I (10 mM sodium phosphate buffer, pH 7.2) or buffer II (PBS; 1.5 mM KH_2PO_4, 2.7 mM KCl, 8.1 mM Na_2HPO_4, 135 mM NaCl, pH 7.2). Several wells were kept untreated as a control for monitoring bacterial growth. Inhibition of growth was determined by measuring the absorbance at 620 nm using a Versa-Max microplate Elisa Reader (Molecular Devices, Sunnyvale, CA, USA) after incubation for 18–24 h at 37 °C. The MIC is defined as the minimal peptide concentration that inhibits bacterial growth.

Antifungal Activity

The fungal strains *Candida albicans* (KCTC 7270) and *Trichosporon beigelli* (KCTC 7707) were used to evaluate the antifungal activity of the test peptides by MTT assay [14]. Briefly, fungal cells (2×10^5 CFU/ml) that were grown in 100 μl of yeast peptone dextrose (YPD) media (dextrose 2%, peptone 1%, yeast extract 0.5%, pH 5.0–5.5) were seeded in each well of a microtiter plate containing 100 μl of twofold serially diluted peptides in buffer I or buffer II (as described above). The plate was then incubated for 24 h at 28 °C. After completion of the desired incubation, 5 μl of MTT solution (5 mg/ml MTT in PBS, pH 7.4) was added to each well, after which the plates were further incubated at 37 °C for 4 h. Next, 30 μl of 20% SDS (w/v) containing 0.02 M HCl was added, and the plates were subsequently incubated at 37 °C for 16 h to dissolve the formazan crystals that had formed. The optical density of each well was measured at 580 nm using a microplate Elisa Reader. All activity assays were performed in triplicate.

Human Red Blood Cell (hRBC) Hemolysis

Hemolytic activities were assessed for the test peptides using hRBCs collected in heparin from healthy donors. The fresh hRBCs were washed three times in PBS via centrifugation at 800 × *g* for 10 min and then resuspended in PBS. After washing, the peptides were dissolved in PBS and added to 100 μl of stock hRBCs suspended in PBS (final RBC concentration, 8% v/v). The samples were then incubated with gentle agitation for 60 min at 37 °C, after which they were centrifuged for 10 min at 800 × *g*. Next, the absorbance of the supernatants was recorded at 414 nm. In addition, controls for zero hemolysis (blank) and 100% hemolysis that were composed of hRBCs suspended in PBS and 1% Triton X-100, respectively, were also analyzed. Melittin (hemolytic peptide) was used as positive control. Each measurement was conducted in triplicate.

CD Spectroscopy

CD spectra were recorded at 25 °C on a Jasco 810 spectropolarimeter (Jasco, Tokyo, Japan) equipped with a temperature control unit using a 0.1-cm path-length quartz cell. The CD spectra of the 50 μM peptides were obtained in different environments, including 10 mM sodium phosphate buffer, 50% TFE, EYPC and EYPG. Ten millimoles sodium phosphate buffer was used to prepare the 50% TFE, EYPC and EYPG. At least five scans in the 250–190 nm wavelength range were conducted and the average blank spectra were subtracted from the average of the sample spectra. All CD spectra are presented as the mean residue ellipticity, $[\theta]_{MRW}$, in deg cm^2/dmol. The α-helical content was determined from the mean residue ellipticities at 222 nm, as indicated in Eqn (1) [15]:

$$\%\ \text{Helix} = ([\theta]_{obs} \times 100)/\{[\theta]_{helix} \times (1 - 2.57/l)\} \qquad (1)$$

where, $[\theta]_{obs}$ is the mean residue ellipticity observed experimentally at 222 nm, $[\theta]_{helix}$ is the ellipticity of a peptide of infinite length with a 100% helix population, taken as 39 500 deg cm^2/dmol, and *l* is the peptide length or, more precisely, the number of peptide bonds.

Calcein Leakage from Liposomes

Calcein-entrapped LUVs composed of EYPE/EYPG (7 : 3, w/w) or EYPC/CH (10 : 1, w/w) were prepared by vortexing the dried lipid in dye buffer solution (70 mM calcein, 10 mM sodium phosphate buffer, pH 7.4). The suspension was freeze-thawed in liquid nitrogen for nine cycles and then extruded 15 times through polycarbonate filters (two stacked 0.2 μM pore size filters) using an *Avanti* Mini-Extruder (Avanti Polar Lipids Inc., Alabaster, AL). Calcein-entrapped vesicles were separated from free calcein by gel filtration chromatography on a Sephadex G-50 column. Entrapped LUVs in a suspension containing 70 μM lipids were then incubated with various concentrations of the peptide (1–12 μM) for 25 min. The fluorescence of the released calcein was assessed using a spectrofluorometer (Perkin-Elmer LS55, Mid Glamorgan, UK) at an

Journal of PeptideScience

excitation wavelength of 480 nm and an emission wavelength of 520 nm. Complete (100%) release was achieved via the addition of 0.1% Triton X-100. Spontaneous leakage was determined to be negligible at this time scale. All experiments were conducted at 25 °C and the apparent percentage of calcein release was calculated according to the following equation [16]:

$$\text{Release (\%)} = 100 \times (F - F_o)/(F_t - F_o) \quad (2)$$

in which F and F_t represent the fluorescence intensity prior to and after the addition of the detergent, respectively, and F_o represents the fluorescence of the intact vesicles.

Computational Modeling and Molecular Dynamics

Modeled structures of the peptides were constructed using the Molecular Operating Environment software (MOE, 2009.10). Full energy minimizations were run for both the parent and the HPA3NT3-analog peptide using the MMF94x force field available in MOE until the RMSD gradient values were below 0.001.

The GROMACS program with the all-atom parameter set was used for all MD simulations [17]. Before starting the dynamics simulations, each system was energy-minimized using the steepest descent algorithm for 100 steps. In all simulations, the temperature and pressure were kept close to the intended values (300 K and 1 bar) using the Berendsen algorithm [18], with $\tau_T = 0.1$ ps and $\tau_p = 0.5$ ps, respectively. The GROMOS96 force field [19] was used to describe the peptide. Simulations were run with a 2-fs time steps. Bond length was constrained using the LINCS algorithm [20]. Lennard–Jones interactions were calculated using a 0.9/1.4-nm twin-range cut off. The short-range electrostatic interactions were calculated to 1.0 nm, and the Particle Mesh Ewald algorithm was used for the long-range interactions [21]. The peptide structures were solvated in TFE, which was parameterized according to Fioroni *et al*. [22]. Both peptides reached equilibrium after 650 ps, and the averaged structure extracted from the last 350 ps was further minimized using an MMF94x force field.

Results and Discussion

An HPA3NT3-analog peptide was designed by substituting Trp with Leu residues (positions 12, 14) and the substitution of Lys residues for Asn and Arg residues (positions 3, 13) within the HPA3NT3 peptide, which was derived from HP (2–20) [10]. In addition, the HPA3NT3-analog had an amidated *C*-terminus, which increased its positive charge by one to enhance the initial binding to the negatively charged bacterial membranes [11].

The MIC values of the peptides against bacterial and fungal strains under low salt (without NaCl) and high salt (with 150 mM NaCl) conditions are summarized in Table 1. The HPA3NT3-analog peptide showed similar activity against *P. aeruginosa* under both low and high salt conditions. Furthermore, the analog peptide displayed twofold enhanced activity against *S. typhimurium* under low salt conditions, but not under high salt conditions. These findings suggest that the HPA3NT3-analog peptide had a certain degree of selectivity for some Gram-negative bacteria. Conversely, the HPA3NT3-analog peptide showed a twofold decrease in antibacterial activity against *E. coli* and Gram-positive bacteria when compared to that shown by the HPA3NT3 peptide, regardless of the salt conditions. This probably occurred because the peptide lacked two tryptophan indole rings that were packed against the HPA3NT3 peptide backbone (Figure 1A). These conformations are required for the insertion of the peptide into the bacterial lipid membrane [23]. In addition, Arg residues have a more dispersed positive charge and higher stability than Lys, which may enhance hydrogen bonding interaction between peptides and the negatively charged bacterial membrane surfaces [24,25]. As a result, the use of Arg residues may have provided tolerance to high salt conditions [26]. These findings are supported by the twofold decrease in activity against bacteria that occurred when the HPA3NT3-analog peptide was evaluated in high salt buffer. However, the increase in the net charge of HPA3NT3-analog from +7 to +9 did not make the peptide more active *in vitro*. This outcome was corroborated by the results of a previous study in which enhancement of the total cationic charge was found to lead to decreased antibacterial activity [27].

Table 1. MICs of the HPA3NT3 and analog peptide against microorganisms in different buffer conditions

	MIC (μM)			
	HPA3NT3		HPA3NT3-analog	
Microorganisms	Buffer I[a]	Buffer II[b]	Buffer I	Buffer II
Gram (−) bacteria				
E. coli	4	4	8	8
S. typhimurium	2	2	1	2
P. aeruginosa	2	2	2	2
Gram (+) bacteria				
S. aureus	4	8	8	16
B. subtilis	4	8	8	16
L. monocytogenes	2	4	4	8
Fungal strains				
C. albicans	8	32	4–8	32
T. beigelli	2–4	2	1	2

[a] Buffer I: 10 mM sodium phosphate buffer, pH 7.2.
[b] Buffer II: phosphate buffered saline (1.5 mM KH_2PO_4, 2.7 mM KCl, 8.1 mM Na_2HPO_4, 135 mM NaCl), pH 7.2.

The results against fungal strains indicated that the HPA3NT3-analog peptide displayed twofold greater antifungal activity than the HPA3NT3 peptide in low salt, while they had similar antifungal activities under high salt conditions. The increased cationicity in the HPA3NT3-analog peptide slightly enhanced the activity against the fungal strains, which is also similar to the findings of other studies [28–30].

The hemolytic activities of these two peptides were assessed against hRBCs to determine the toxicity toward higher eukaryotic cells. The HPA3NT3-analog peptide caused minimal hemolysis (4.2%) against hRBCs, while HPA3NT3 induced 71% hemolysis at 200 μM (Figure 2). These findings clearly demonstrate that the substitution of amino acids and increased cationicity in the HPA3NT3-analog peptide led to decreased hemolysis. The enhancement of positive charge is always connected with reduced hydrophobicity and leads to a modification of hydrophobic moment [31]. Therefore, these modifications can govern the activity of AMPs and lead to greatly reduced hemolytic activity [32].

The CD spectra of the peptides in buffer, 50% TFE, EYPG and EYPC were also analyzed (Figure 3A, B). Both peptides were found to have a random coil structure in aqueous solution. The CD spectra

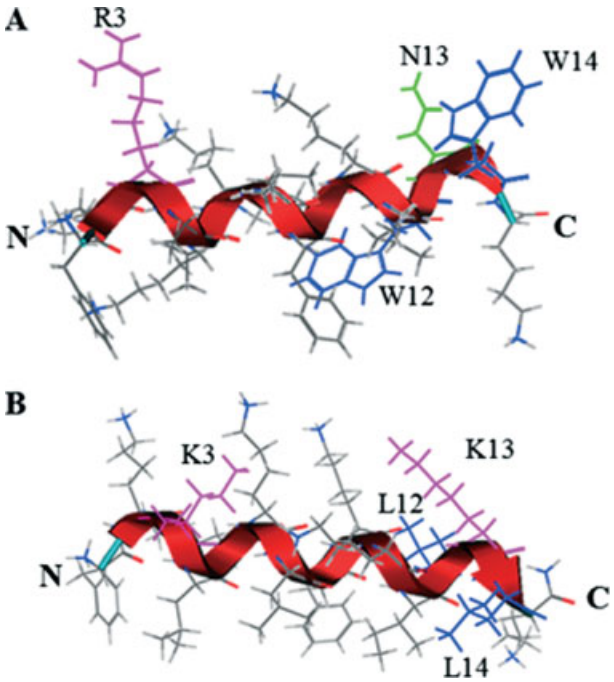

Figure 1. The lowest energy structures of peptides among the 20 final structures. The helix is shown in red. Ribbon diagram of the peptides structure: HPA3NT3 (A): HPA3NT3-analog (B). The Trp and Leu are shown in blue; Arg and Lys are shown in pink; Asn is in green.

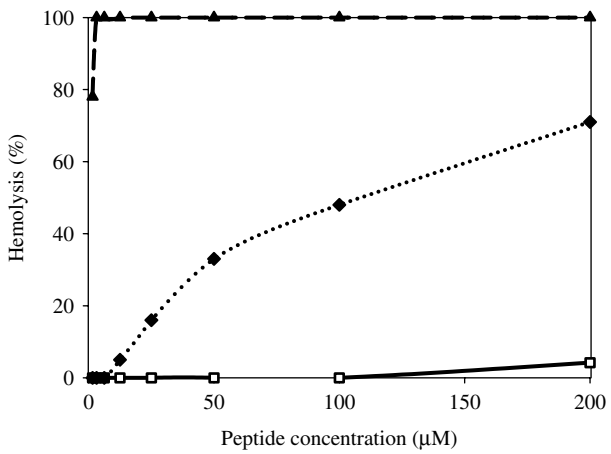

Figure 2. Hemolytic activities of the peptides against human erythrocytes. HPA3NT3 (♦), HPA3NT3-analog (□), and Melittin (▲).

of HPA3NT3 and the HPA3NT3-analog had an α-helical structure in 50% TFE and EYPG. However, the HPA3NT3-analog showed increased helical content in EYPG micelles when compared to HPA3NT3. This was likely due to its greater length and longer helical segments. These findings indicate that a more helical HPA3NT3-analog would be more stable than HPA3NT3 because substitution of the amino acids may induce helical stacking in multimers.

The HPA3NT3-analog peptide did not bind to zwitterionic EYPC vesicles, which is consistent with their lack of hemolytic activity in erythrocytes [6,33,34]. However, the HPA3NT3 peptide adopted an ordered structure in the presence of EYPC, which caused a dramatic shift in binding conformation from 198 nm (buffer)

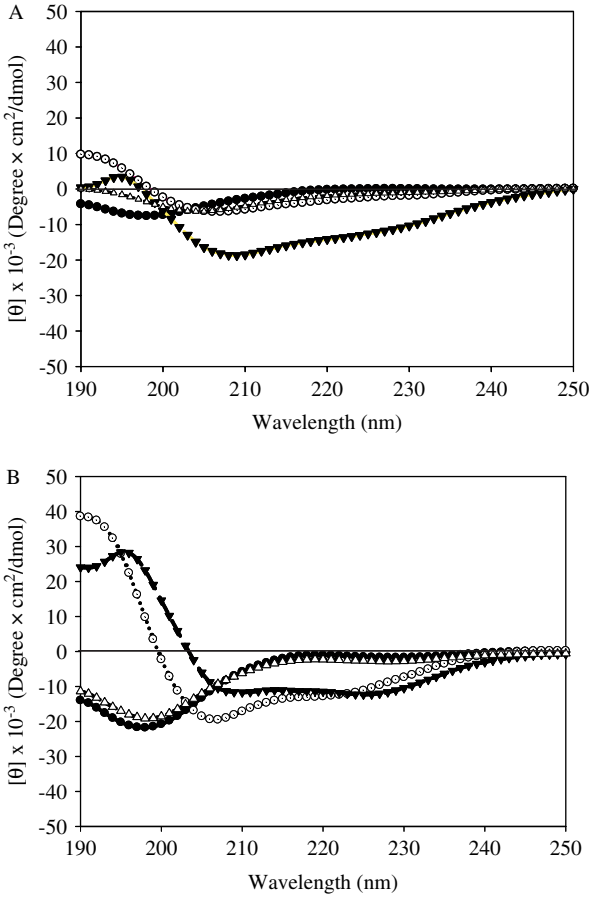

Figure 3. CD spectra of the HPA3NT3 (A) and HPA3NT3-analog (B) in the presence of 10 mM sodium phosphate buffer (pH 7.2) (●), 50% TFE (⊙), EYPG (▼), and EYPC (△).

to 204 nm. This change may be attributed to the Trp and Arg side chain of HPA3NT3 and likely correlates with the observed increased hemolysis against erythrocytes.

The fact that Trp residues have a preference for the binding of peptides to the membrane interfacial region has been well documented [35,36]. For example, Aliste *et al*. [37] reported that the Trp residue can associate with the positively charged choline head groups of lipid bilayers. In addition, several studies have shown that the presence of Trp residues in AMPs (including melittin) is responsible for hemolytic activity [4,6,38,39]. The guanidinium group of Arg side chains also promotes interaction with the phosphate group of zwitterionic phospholipids such as phosphatidyl choline, which has been found to be responsible for the hemolytic activity of AMPs [5]. Moreover, the results of other studies have suggested that the replacement of Arg with Lys did not substantially alter peptide binding to the anionic membrane but moderately decreased binding to the zwitterionic membrane [5,33,40]. These phenomena likely occurred in our study in response to the substitutions of Trp and Arg with Leu and Lys, respectively. Specifically, these changes likely caused the HPA3NT3-analog to become less selective to the zwitterionic membrane.

We also determined the ability of the peptides to cause the leakage of calcein from EYPE/EYPG (7 : 3 w/w) vesicles, which mimic bacterial membranes. Treatment of liposomes composed of EYPE/EYPG (7 : 3 w/w) vesicles with HPA3NT3 at 4 μM was

Journal of PeptideScience

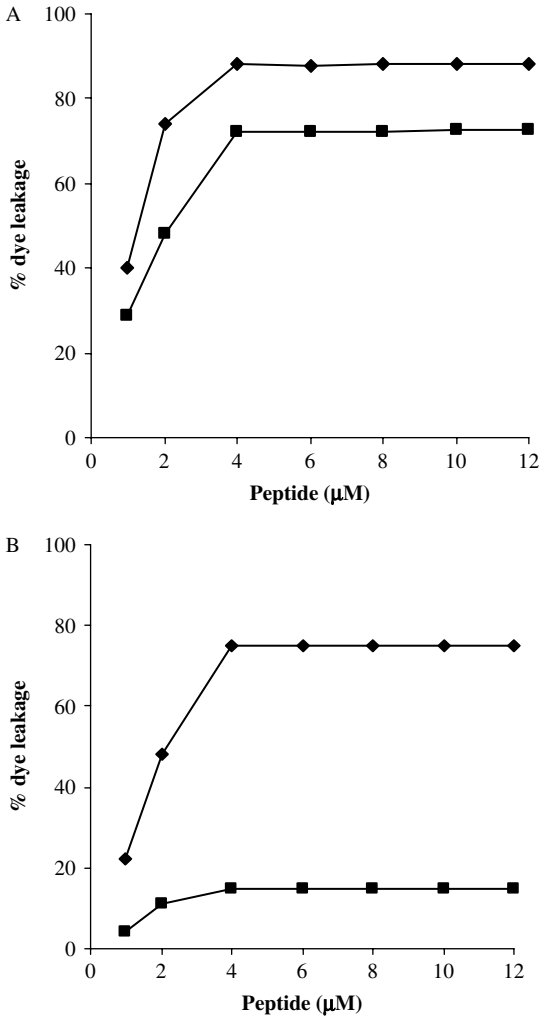

Figure 4. Calcein leakage from EYPE : EYPG (7 : 3, w/w) (A), and EYPC : CH (9 : 1,w/w) (B) induced by peptides: HPA3NT3 (♦), HPA3NT3-analog (■).

found to disrupt 88% of the vesicles. Treatment with the same concentration of the HPA3NT3-analog resulted in the release of 72% of the entrapped calcein (Figure 4A). When the activity of HPA3NT3 against liposomes composed of zwitterionic EYPC/CH (10 : 1 w/w) was evaluated, almost 79% of the calcein was released from these vesicles at 4 μM. Treatment with the same concentration of the HPA3NT3-analog resulted in the release of 22% of the total entrapped calcein because of surface interaction (Figure 4B). These results suggest that the presence of Trp and Arg in the HPA3NT3 resulted in a dramatic increase in the extent of release, which is consistent with the observed hemolytic activity of HPA3NT3 peptide (Figure 2). The effects of HPA3NT3-analog were comparable to those of HPA3NT3 peptide in terms of their mechanism of action against bacterial membranes.

The ribbon diagram representation of the modeling structure of peptides with the lowest total energy among the final 20 structures is shown in Figure 1A and B. In the HPA3NT3-analog peptide, four positively charged lysine residues are concentrated on the hydrophilic face, forming a hydrophilic patch (Figure 1B). This indicates that the amphipathic structure was improved, which likely resulted in decreased hemolysis and enabled increased binding with EYPG vesicles. Homology based modeling structures of the HPA3NT3 and HPA3NT3-analog peptide were used for MD

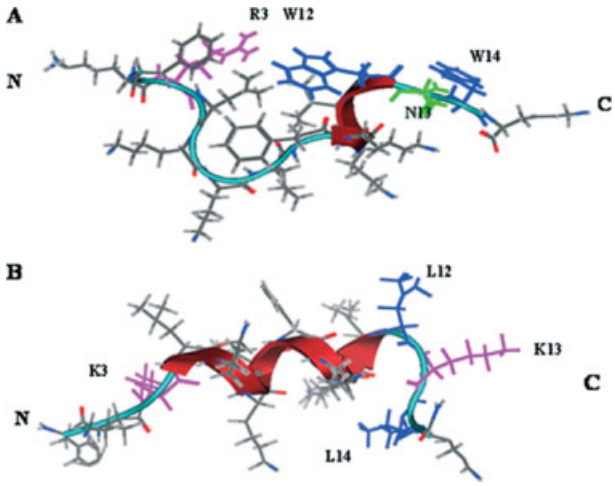

Figure 5. Minimized average structure over the last 350 ps of simulation at 300 K for HPA3NT3 (A) and HPA3NT3-analog (B) in TFE. The Trp and Leu are shown in blue; Arg and Lys are shown in pink; Asn is in green.

studies under the TFE/water mixture condition. Both peptides showed distinct structural changes when associated with the TFE/water mixture (Figure 5A, B). However, the HPA3NT3-analog was found to form a more uniform helix from residues 4–11, while HPA3NT3 formed a single helical turn between residues 9 and 12. The MD simulation structures were in agreement with the CD structure of these peptides in 50% TFE.

Conclusions

In conclusion, the substitution of Trp with Leu and Arg and Asn with Lys resulted in a slight change in the activity of the HPA3NT3-analog against the bacterial membrane and a significant decrease in hemolytic activity in addition to an increase in cationicity and the substitution of amino acids, which resulted in low binding to zwitterionic membranes. However, the basic mechanism of action of this HPA3NT3-analog peptide did not change, as demonstrated by the calcein leakage study. Furthermore, a comparison of the MD structures of these peptides revealed that amino acid substitutions induced significant variation in the peptide structure. The structural differences in these peptides likely contributed to their hemolytic activity in EYPC vesicles.

Acknowledgements

This work was supported by the Pioneer Research Program for Converging Technology of the Ministry of Education, Science and Technology, Republic of Korea (Grant No. M1071118001-08M1118-00110) (2009).

References

1 Hancock RE. Cationic peptides: effectors in innate immunity and novel antimicrobials. *Lancet Infect Dis.* 2001; **1**: 156–164.
2 Brown KL, Hancock RE. Cationic host defense (antimicrobial) peptides. *Curr. Opin. Immunol.* 2006; **18**: 24–30.
3 Zasloff M. Antimicrobial peptides of multicellular organisms. *Nature* 2002; **415**: 389–395.
4 Rozek A, Friedrich CL, Hancock RE. Structure of the bovine antimicrobial peptide indolicidin bound to dodecylphosphocholine and sodium dodecyl sulfate micelles. *Biochemistry* 2000; **39**: 15765–15774.

5 Yang ST, Shin SY, Lee CW, Kim YC, Hahm KS, Kim JI. Selective cytotoxicity following Arg-to-Lys substitution in tritrpticin adopting a unique amphipathic turn structure. *FEBS Lett.* 2003; **540**: 229–233.
6 Hawrani A, Howe RA, Walsh TR, Dempsey CE. Origin of low mammalian cell toxicity in a class of highly active antimicrobial amphipathic helical peptides. *J. Biol. Chem.* 2008; **283**: 18636–18645.
7 Dathe M, Wieprecht T. Structural features of helical antimicrobial peptides: their potential to modulate activity on model membranes and biological cells. *Biochim. Biophys. Acta* 1999; **1462**: 71–87.
8 Giangaspero A, Sandri L, Tossi A. Amphipathic alpha helical antimicrobial peptides. *Eur. J. Biochem.* 2001; **268**: 5589–5600.
9 Bylund J, Christophe T, Boulay F, Nyström T, Karlsson A, Dahlgren C. Proinflammatory activity of a cecropin-like antibacterial peptide from *Helicobacter pylori*. *Antimicrob. Agents Chemother.* 2001; **45**: 1700–1704.
10 Park SC, Kim MH, Hossain MA, Shin SY, Kim Y, Stella L, Wade JD, Park Y, Hahm KS. Amphipathic alpha-helical peptide, HP (2–20), and its analogues derived from *Helicobacter pylori*: pore formation mechanism in various lipid compositions. *Biochim. Biophys. Acta* 2008; **1778**: 229–241.
11 Shai Y, Oren Z. From ''carpet'' mechanism to de-novo designed diastereomeric cell-selective antimicrobial peptides. *Peptides* 2001; **22**: 1629–1641.
12 Atherton E, Sheppard RC. *Solid Phase Peptide Synthesis: A Practical Approach*. IRL: Oxford, 1989.
13 Park KH, Park Y, Park IS, Hahm KS, Shin SY. Bacterial selectivity and plausible mode of antibacterial action of designed Pro-rich short model antimicrobial peptides. *J. Pept. Sci.* 2008; **14**: 876–882.
14 Jahn B, Martin E, Stueben A, Bhakdi S. Susceptibility testing of *Candida albicans* and *Aspergillus* species by a simple microtiter menadione-augmented 3-(4,5-dimethyl-2-thiazolyl)-2,5-diphenyl-2H-tetrazolium bromide assay. *J. Clin. Microbiol.* 1995; **33**: 661–667.
15 Chen YH, Yang JT, Chau KH. Determination of the helix and β form of protein in aqueous solution by circular dichroism. *Biochemistry* 1974; **13**: 3350–3359.
16 Matsuzaki K, Sugishita K, Miyajima K. Interactions of an antimicrobial peptide, magainin 2, with lipopolysaccharide-containing liposomes as a model for outer membranes of Gram-negative bacteria. *FEBS Lett.* 1999; **449**: 221–224.
17 Lindahl E, Hess B, Van der Spoel D. GROMACS 3.0: a package for molecular simulation and trajectory analysis. *J. Mol. Model.* 2001; **7**: 306–317.
18 Berendsen CD, Postma JPM, Van Gunsteren WF, DiNola A, Haak JR. Molecular dynamics with coupling to an external bath. *J. Chem. Phys.* 1984; **81**: 3684–3690.
19 Van Gunsteren WF, Billeter SR, Eising AA, Hünenberger PH, Krüger P, Mark AE, Scott WRP, Tironi IG. *Biomolecular Simulations: The GROMOS96 Manual and User Guide*. Zürich VdF Hochschulverlag ETHZ: Groningen, 1996.
20 Hess B, Bekker H, Berendsen HJC, Fraaije JGEM. LINCS: a linear constraint solver for molecular simulations. *J. Comput. Chem.* 1997; **18**: 1463–1472.
21 Darden T, York D, Pedersen LG. Particle mesh Ewald: an N. log (N) method for Ewald sums in large systems. *J. Chem. Phys.* 1993; **98**: 10089–10092.
22 Fioroni M, Burger K, Mark AE, Roccatano D. A new 2,2,2-trifluoroethanol model for molecular dynamics simulations. *J. Phys. Chem. B* 2000; **104**: 12347–12354.
23 Wei SY, Wu JM, Kuo YY, Chen HL, Yip BS, Tzeng SR, Cheng JW. Solution structure of a novel tryptophan-rich peptide with bidirectional antimicrobial activity. *J. Bacteriol.* 2006; **188**: 328–334.
24 Schibli DJ, Montelaro RC, Vogel HJ. The membrane-proximal tryptophan-rich region of the HIV glycoprotein, gp41, forms a well defined helix in dodecylphosphocholine micelles. *Biochemistry* 2001; **40**: 9570–9578.
25 Vogel HJ, Schibli DJ, Jing W, Lohmeier-Vogel EM, Epand RF, Epand RM. Towards a structure-function analysis of bovine lactoferricin and related tryptophan-and arginine-containing peptides. *Biochem. Cell Biol.* 2002; **80**: 49–63.
26 Muhle SA, Tam JP. Design of Gram-negative selective antimicrobial peptides. *Biochemistry* 2001; **40**: 5777–5785.
27 Zhu WL, Song YM, Park Y, Park KH, Yang ST, Kim JI, Park IS, Hahm KS, Shin SY. Substitution of the leucine zipper sequence in melittin with peptoid residues affects self-association, cell selectivity, and mode of action. *Biochim. Biophys. Acta* 2007; **1768**: 1506–1517.
28 Rothstein DM, Spacciapoli P, Tran LT, Xu T, Roberts FD, Dalla Serra M, Buxton DK, Oppenheim FG, Friden P. Anticandida activity is retained in P-113, a 12-amino-acid fragment of histatin 5. *Antimicrob. Agents Chemother.* 2001; **45**: 1367–1373.
29 Sonesson A, Ringstad L, Nordahl EA, Malmsten M, Mörgelin M, Schmidtchen A. Antifungal activity of C3a and C3a-derived peptides against *Candida*. *Biochim. Biophys. Acta* 2007; **1768**: 346–353.
30 Zelezetsky I, Tossi A. Alpha-helical antimicrobial peptides-using a sequence template to guide structure-activity relationship studies. *Biochim. Biophys. Acta* 2006; **1758**: 1436–1449.
31 Kiyota T, Lee S, Sugihara G. Design and synthesis of amphiphilic alpha-helical model peptides with systematically varied hydrophobic-hydrophilic balance and their interaction with lipid- and bio-membranes. *Biochemistry* 1996; **35**: 13196–13204.
32 Dathe M, Nikolenko H, Meyer J, Beyermann M, Bienert M. Optimization of the antimicrobial activity of magainin by modification of charge. *FEBS Lett.* 2001; **501**: 146–150.
33 Andrä J, Monreal D, Martinez de Tejada G, Olak C, Brezesinski G, Gomez SS, Goldmann T, Bartels R, Brandenburg K, Moriyon I. Rationale for the design of shortened derivatives of the NK-lysin-derived antimicrobial peptide NK-2 with improved activity against Gram-negative pathogens. *J. Biol. Chem.* 2007; **282**: 14719–14728.
34 Glukhov E, Stark M, Burrows LL, Deber CM. Basis for selectivity of cationic antimicrobial peptides for bacterial versus mammalian membranes. *J. Biol. Chem.* 2005; **280**: 33960–33967.
35 Yau WM, Wimley WC, Gawrisch K, White SH. The preference of tryptophan for membrane interfaces. *Biochemistry* 1998; **37**: 14713–14718.
36 Persson S, Killian JA, Lindblom G. Molecular ordering of interfacially localized tryptophan analogs in ester-and ether-lipid bilayers studied by 2H-NMR. *Biophys. J.* 1998; **75**: 1365–1371.
37 Aliste MP, MacCallum JL, Tieleman DP. Molecular dynamics simulations of pentapeptides at interfaces: salt bridge and cation-π interactions. *Biochemistry* 2003; **42**: 8976–8987.
38 Subbalakshmi C, Krishnakumari V, Nagaraj R, Sitaram N. Requirements for antibacterial and hemolytic activities in the bovine neutrophil derived 13-residue peptide indolicidin. *FEBS Lett.* 1996; **395**: 48–52.
39 Falla TJ, Karunaratne DN, Hancock RE. Mode of action of the antimicrobial peptide indolicidin. *J. Biol. Chem.* 1996; **271**: 19298–19303.
40 Andrushchenko VV, Aarabi MH, Nguyen LT, Prenner EJ, Vogel HJ. Thermodynamics of the interactions of tryptophan rich cathelicidin antimicrobial peptides with model and natural membranes. *Biochim. Biophys. Acta* 2008; **1778**: 1004–1014.

